SUPPLEMENTARY DATA

MS_PG-00034-2020_R2: Identification of a peripheral blood gene signature predicting aortic valve calcification

Donal MacGrogan[1,2,*], Beatriz Martínez Poveda[1,2], Jean-Pierre Desvignes[3], Leticia Fernandez-Friera[2,4,5], Manuel José Gomez[6], Eduardo Gil Vilariño[7], Sergio Callejas Alejano[7], Pablo Garcia-Pavia[2,8,9], Jorge Solis[10], Joaquín Lucena[11], David Salgado[3], Gwenaelle Collod-Béroud[3], Emilie Faure[3], Alexis Théron[12], Julia Torrents[13], Jean-François Avierinos[3,12], Lorena Montes[14], Ana Dopazo[7], Valentín Fuster[15,16], Borja Ibañez[2,17], Fátima Sánchez-Cabo[6], Stephane Zaffran[3] & José Luis de la Pompa[1,2,*]

[1] Intercellular Signaling in Cardiovascular Development & Disease laboratory, Centro Nacional de Investigaciones Cardiovasculares Carlos III (CNIC), Melchor Fernández Almagro 3, 28029 Madrid, SPAIN

[2] Ciber de Enfermedades Cardiovasculares, Instituto de Salud Carlos III, Melchor Fernández Almagro 3, 28029 Madrid, SPAIN

[3] Aix Marseille University, MMG, INSERM U1251, Marseille, FRANCE

[4] Translational Laboratory for Cardiovascular Imaging and Therapy, CNIC, SPAIN

[5] HM Hospitales-Centro Integral de Enfermedades Cardiovasculares, Madrid, SPAIN

[6] Bioinformatics Unit, CNIC, SPAIN

[7] Genomics Unit, CNIC, SPAIN

[8] Departmento de Cardiología, Hospital Universitario Puerta de Hierro, Madrid, SPAIN

[9] Universidad Francisco de Vitoria, Pozuelo de Alarcón, Madrid, SPAIN

[10] Departmento of Cardiología, Hospital Universitario Doce de Octubre, Madrid, SPAIN

[11] Servicio de Patología Forense, Instituto de Medicina Legal y Ciencias Forenses, Sevilla, SPAIN

[12] Service de Cardiologie, Hôpital de la Timone, 13005, Marseille, FRANCE

[13] Service d'anatomie et Cytologie Pathologiques, Hôpital de la Timone, 13005, Marseille, FRANCE

[14] Hospital Clínico San Carlos, Madrid, SPAIN

[15] Cardiovascular Imaging and Population Studies Laboratory, CNIC, SPAIN

[16] Cardiology Department, Icahn School of Medicine at Mount Sinai, New York, New York, USA

[17] IIS-Fundación Jiménez Díaz Hospital Universitario, Madrid, SPAIN

* Corresponding authors

Correspondence:
Jose-Luis de la Pompa
Intercellular Signaling in Cardiovascular Development & Disease laboratory
Centro Nacional de Investigaciones Cardiovasculares Carlos III (CNIC)
Melchor Fernández Almagro 3, 28029 Madrid, SPAIN.
Tel: +34 91 4531200
Email: jlpompa@cnic.es

SUPPLEMENTARY FIGURES

Supplementary Figure S1. (A) Gene-expression profile-based principal component analysis (PCA) plot mapping of sample batches. Each point represents a single sample colour-coded according to batch origin. Batch 1 samples (dark blue) are distributed randomly along the first principal component (PC1) axis, whereas batch 2 samples (lighter blue) are distributed along PC2. (B) K-means clustering of genes detected in RNASeq experiments. The average expression profiles of 19,662 genes across six biological conditions were used to define 50 gene clusters. Lines represent scaled RPKM values. Biological conditions are encoded as follows: 9 (foetal 9 wk), 13 (foetal 12-13 wk), 22 (foetal 22 wk), C (adult control samples), B (calcified BAV samples), T (calcified TAV samples). Each cluster contains approximately 400 genes (from 216 to 681 genes). The 6 boxed plots are representative of the 6 expression pattern combinations (see Results). (C) Relative average expression of 10256 genes included in metaclusters MC1-6 and hierarchical clustering of the sample groups based on Euclidean distance.

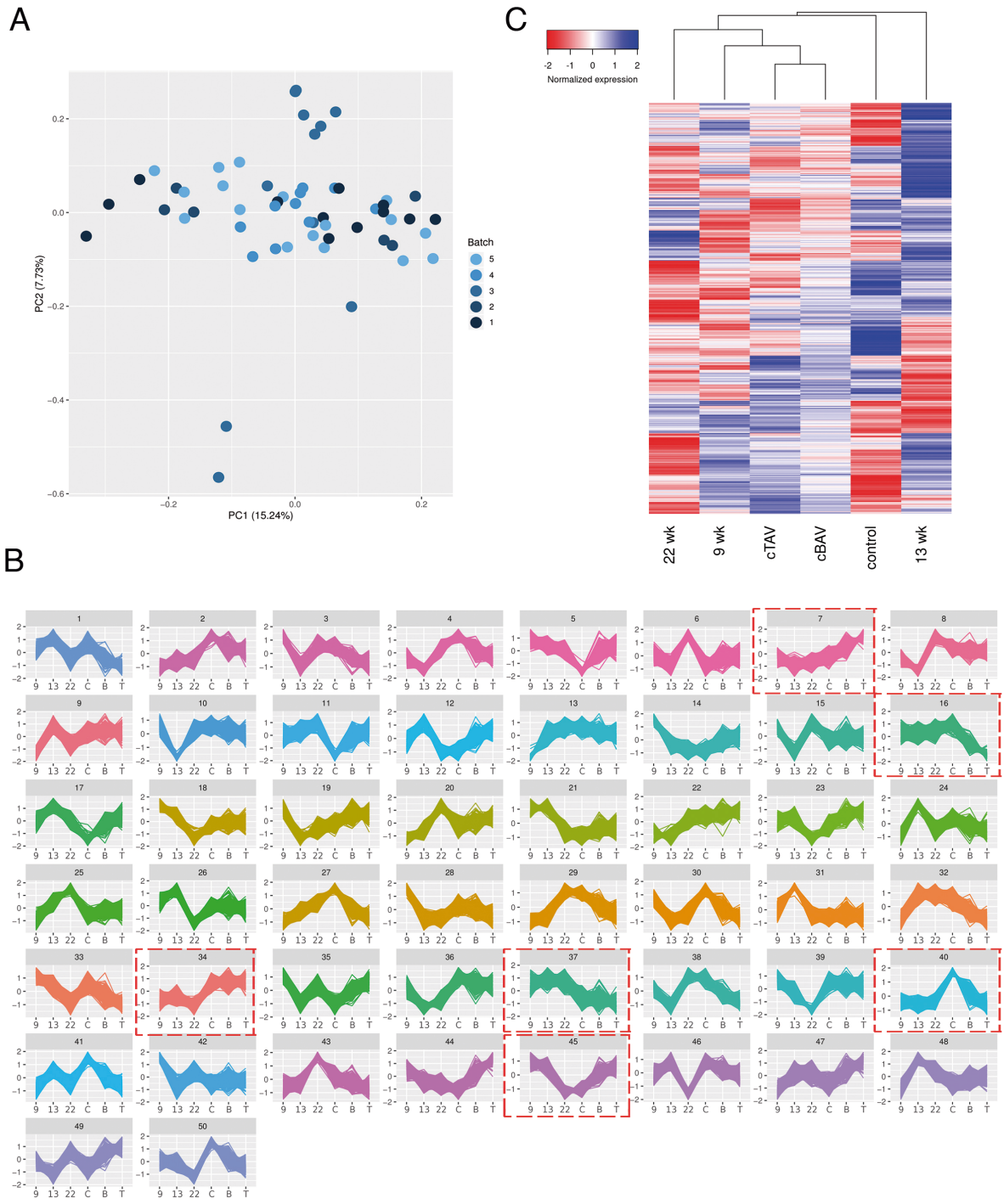

Supplementary_Figure_S1_MacGrogan_et_al

Supplementary Figure S2. Hierarchical clustering of enriched pathways in MC3. IPA results for MC3 identified 168 enriched canonical pathways with a Benjamini-Hochberg adjusted $P<0.05$, which appear listed on the right. The central heatmap represents the percentage of genes shared between pathways (from 0% to 100%). The dendrogram at the top shows pathway relatedness, calculated on the basis of the shared-gene ratios. The heatmap on the left represents mean gene expression for the genes associated with each pathway across biological conditions, on a normalised scale (from -2 to 2 for values below and above the mean, respectively).

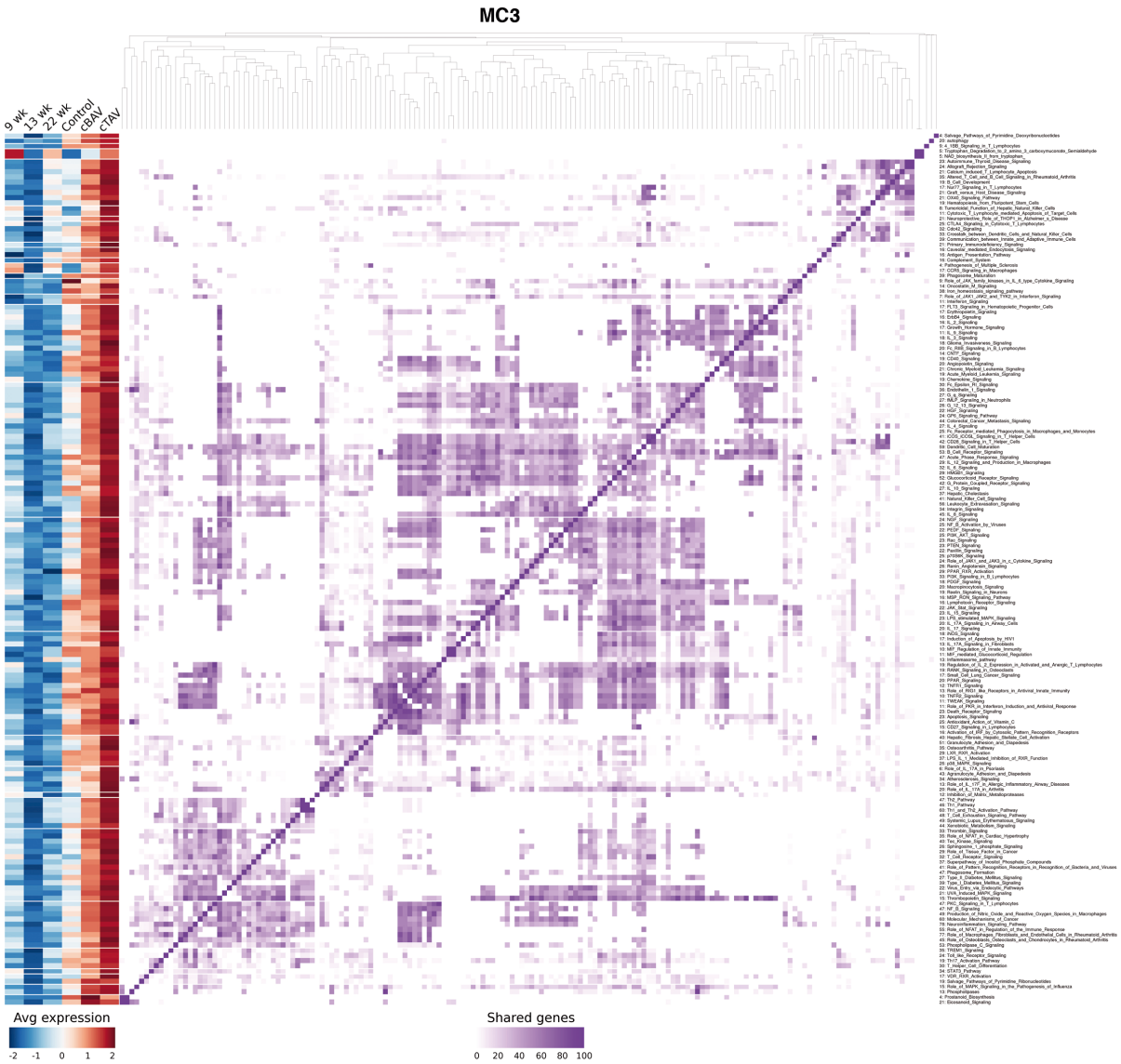

Supplementary_Figure_S2_MacGrogan_et_al

Supplementary Figure S3. Top 5 pathways associated with MC3. Pathways summarized in Figure 3 are involved in innate and adaptive immunity. Heatmaps represent mean expression values for the genes associated with each pathway across biological conditions, on a normalised scale (with negative or positive sign for values below and above the mean, respectively). Gene names and K-means based cluster identifiers appear on the right. Transcripts in MC3 were mainly involved in innate and adaptive immunity.

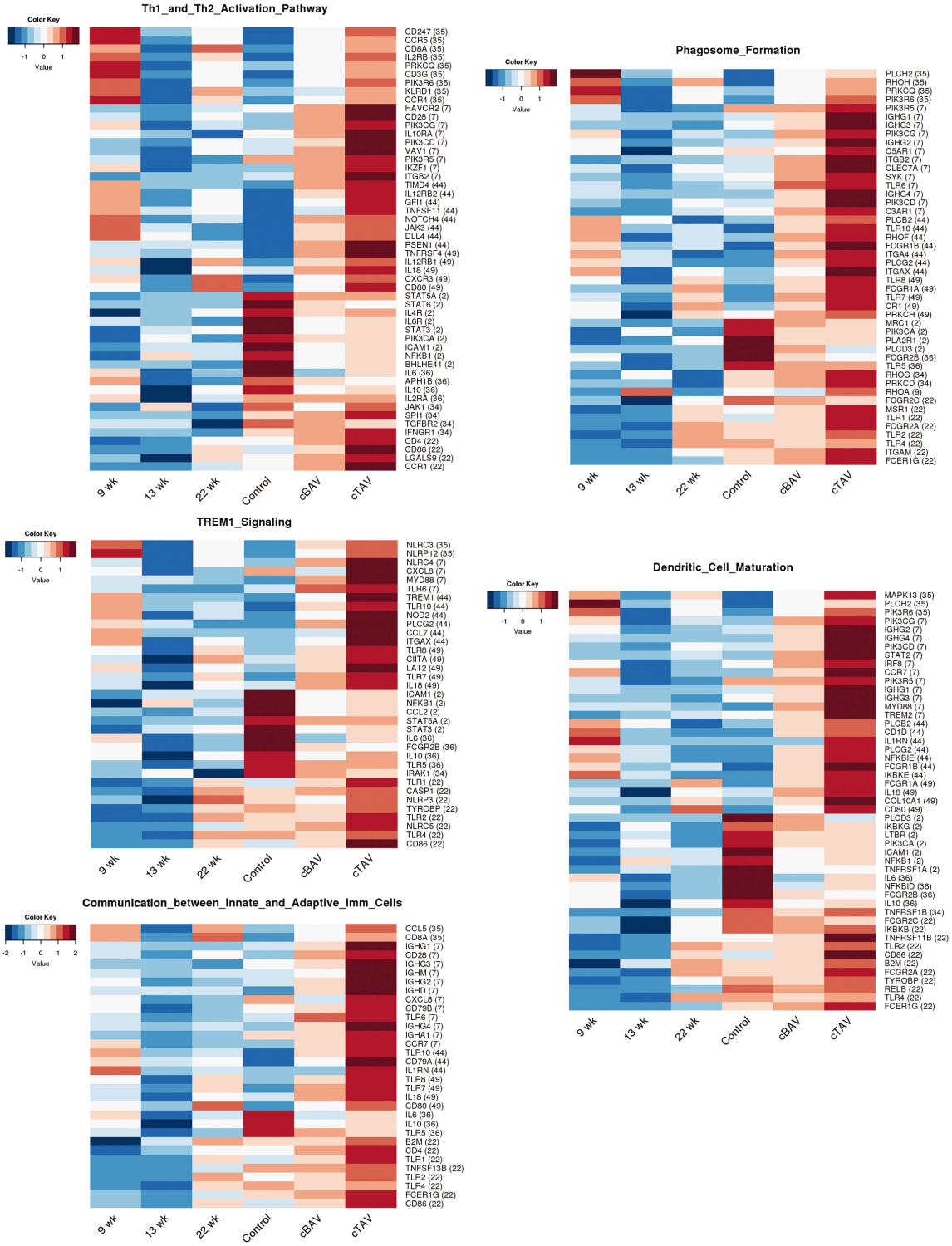

Supplementary_Figure_S3_MacGrogan_et_al

Supplementary Figure S4. Hierarchical clustering of enriched pathways in MC4. IPA results for MC4 identified 202 enriched canonical pathways with a Benjamini-Hochberg adjusted $P<0.05$, which appear listed on the right. The central heatmap represents the percentage of genes shared between pathways (from 0% to 100%). The dendrogram at the top represents pathway relatedness, calculated on the basis of the shared-gene ratios. The heatmap on the left represents mean gene expression for the genes associated with each pathway across biological conditions, on a normalized scale (from -2 to 2, for values below and above the mean, respectively).

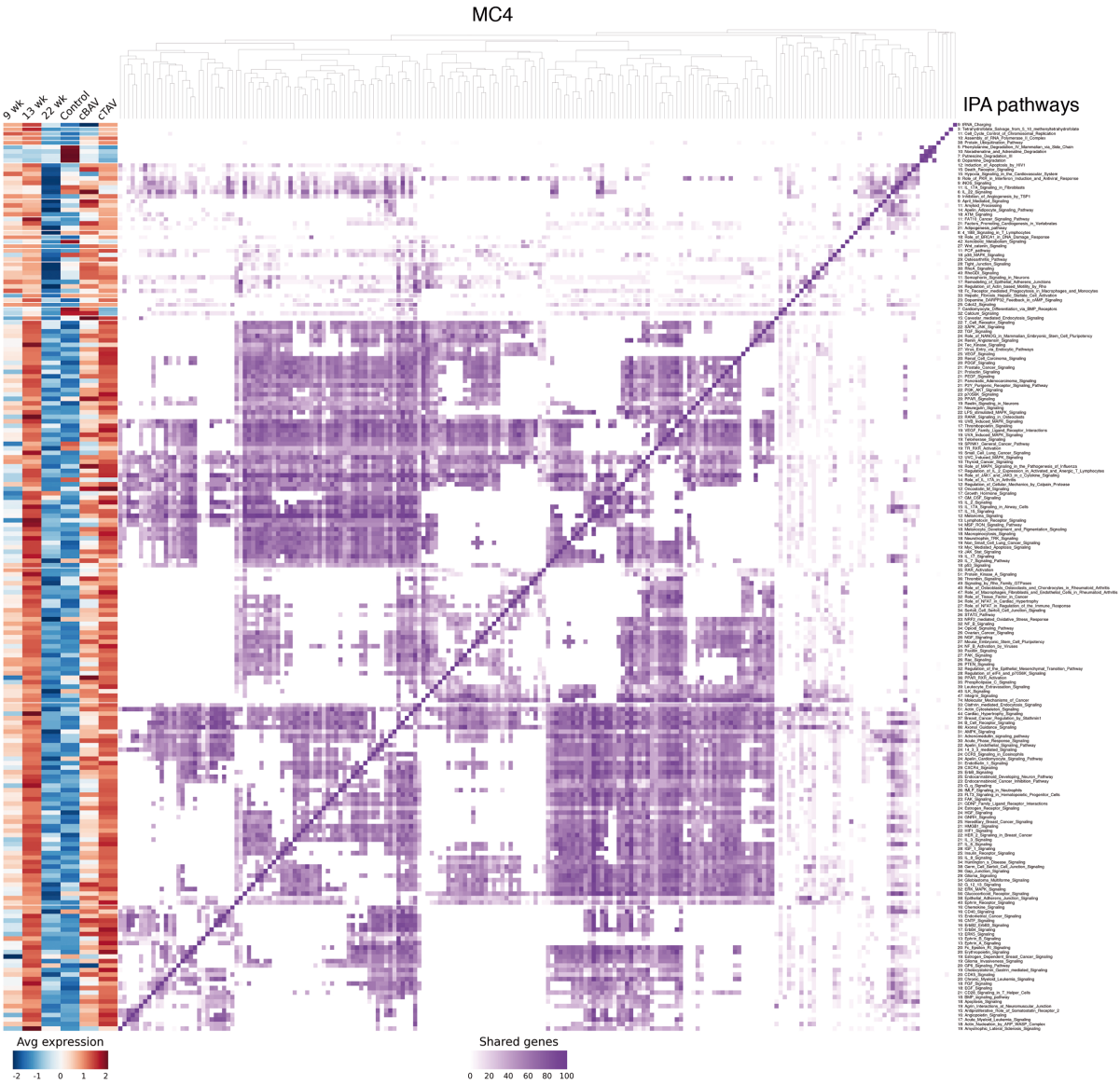

Supplementary_Figure_S4_MacGrogan_et_al

Supplementary Figure S5. Top 5 pathways associated with MC4. Pathways summarized in Figure 3 are involved in cell migration. Heatmaps represent expression values for the genes associated with each pathway across biological conditions, on a normalised scale (with negative or positive sign for values below and above the mean, respectively). Gene names and K-means based cluster identifiers appear on the right.

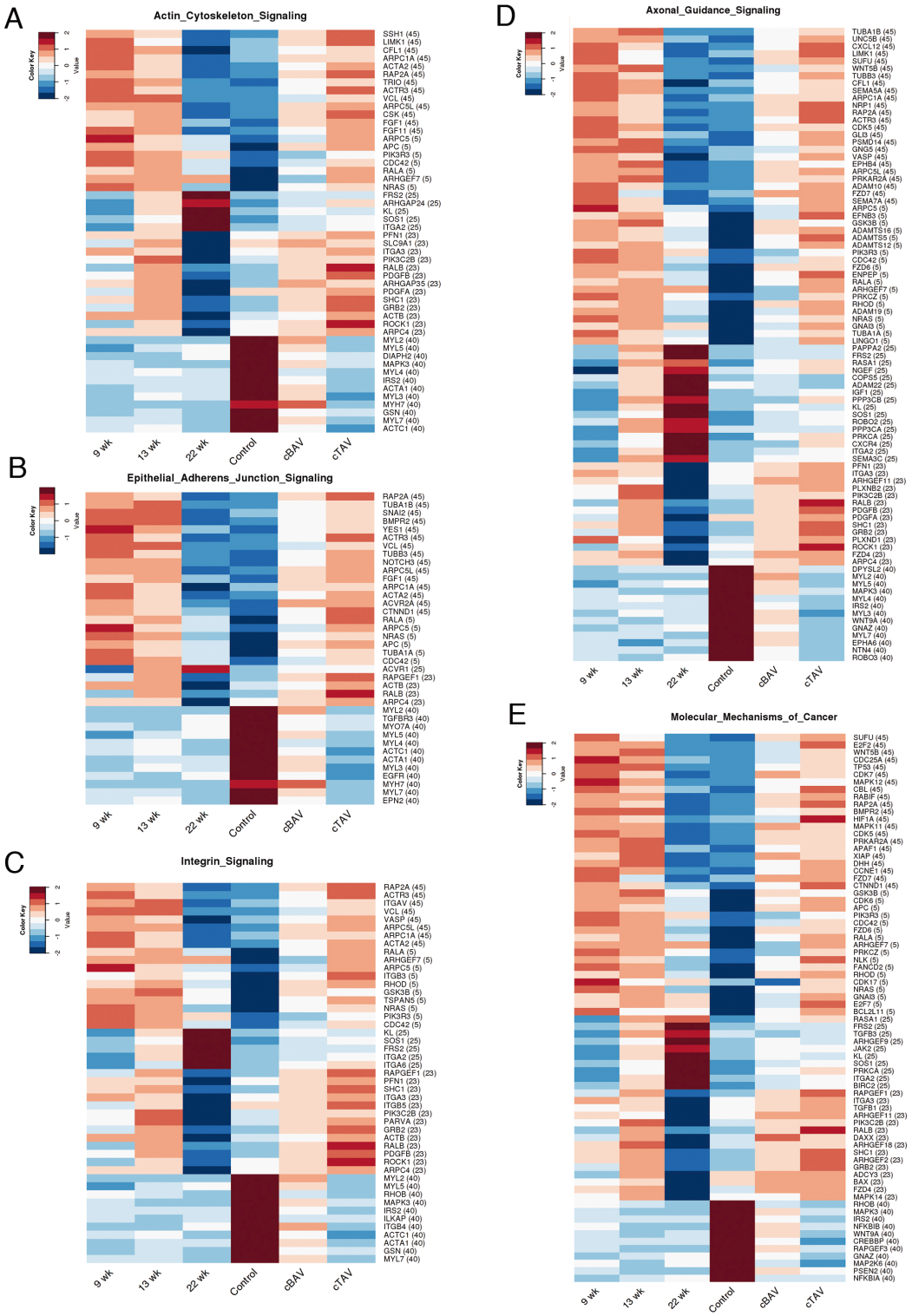

Supplementary_Figure_S5_MacGrogan_et_al

Supplementary Figure S6. (A) Hierarchical clustering of enriched pathways in MC6. IPA results for MC6 identified 23 enriched canonical pathways with a Benjamini-Hochberg adjusted $P<0.05$, which appear listed on the right. The central heatmap represents the percentage of genes shared between pathways (from 0% to 100%). The dendrogram at the top represents pathway relatedness, calculated on the basis of the shared-gene ratio. The heatmap on the left represents mean gene expression for the genes associated with each pathway across biological conditions, on a normalised scale (from -2 to 2, for values below and above the mean, respectively). (B) Top 5 pathways associated with MC6. Pathways summarized in Figure 3 are involved in DNA metabolism. Heatmaps represent expression values for the genes associated with each pathway across biological conditions, on a normalised scale (with negative or positive sign for values below and above the mean, respectively). Gene names and K-means based cluster identifiers appear on the right.

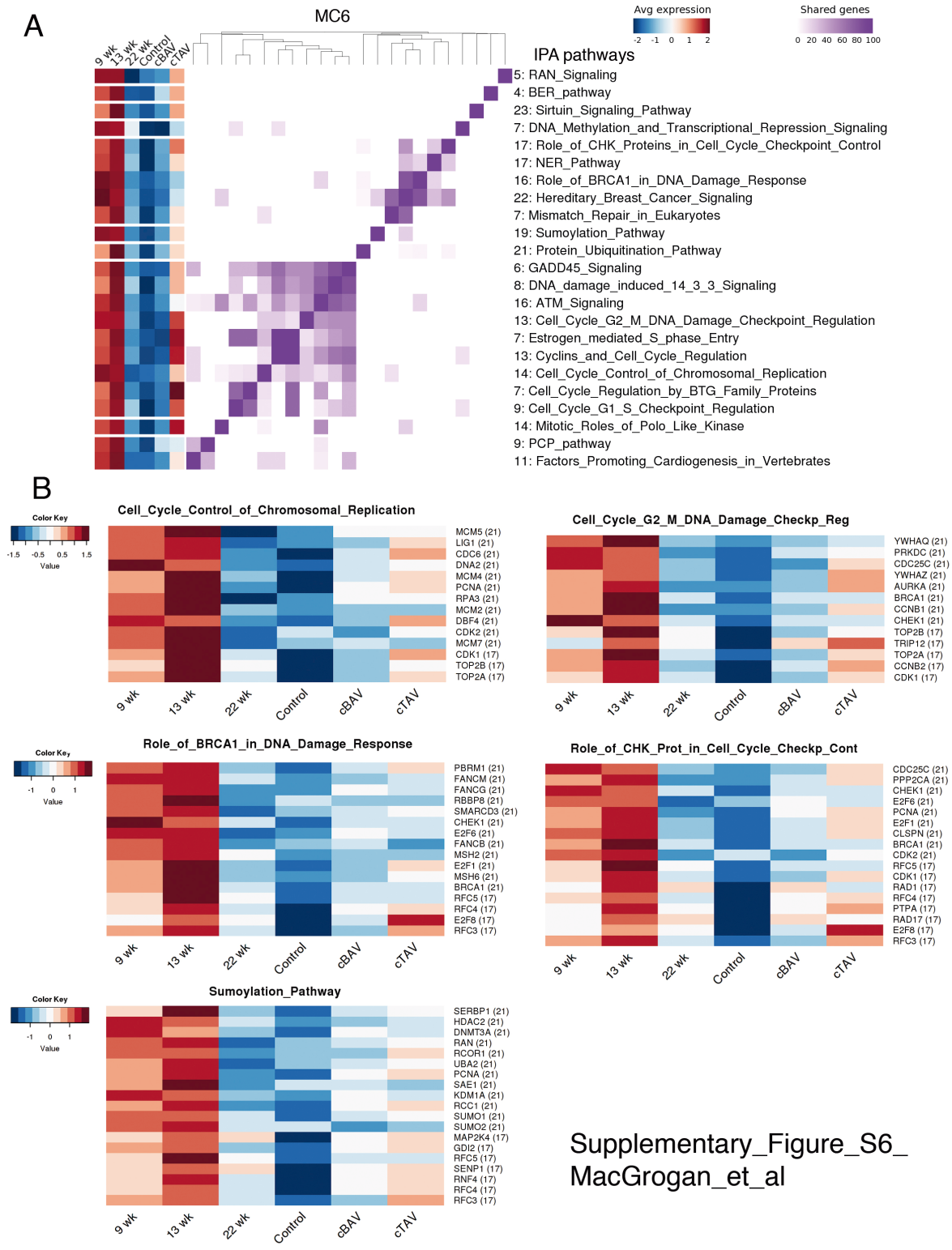

Supplementary_Figure_S6_
MacGrogan_et_al

Supplementary Figure S7. Hierarchical clustering of enriched pathways in MC2. IPA results for MC2 identified 83 enriched canonical pathways with a Benjamini-Hochberg adjusted $P<0.05$, which appear listed on the right. The central heatmap represents the percentage of genes shared between pathways (from 0% to 100%). The dendrogram at the top represents pathway relatedness, calculated on the basis of the shared-gene ratio. The heatmap on the left represents mean gene expression for the genes associated with each pathway across biological conditions, on a normalised scale (from -2 to 2, for values below and above the mean, respectively).

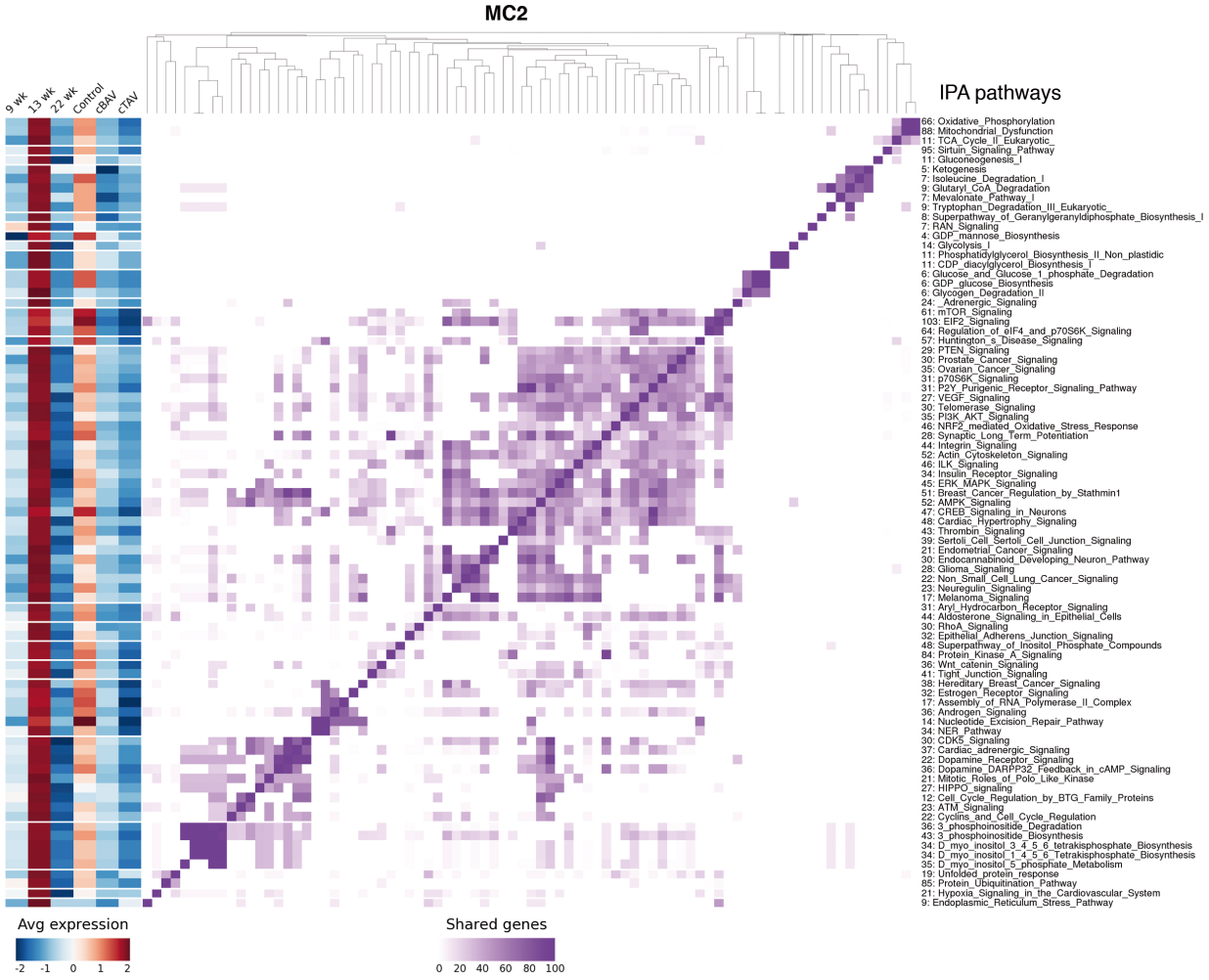

Supplementary_Figure_S7_MacGrogan_et_al

Supplementary Figure S8. Top 5 pathways associated with MC2. Pathways sumarized in Figure 3 are involved in OXPHOS metabolism and ribosome biogenesis. Heatmaps represent expression values for the genes associated with each pathway across biological conditions, on a normalised scale (with negative or positive sign for values below and above the mean, respectively). Gene names and K-means based cluster identifiers appear on the right.

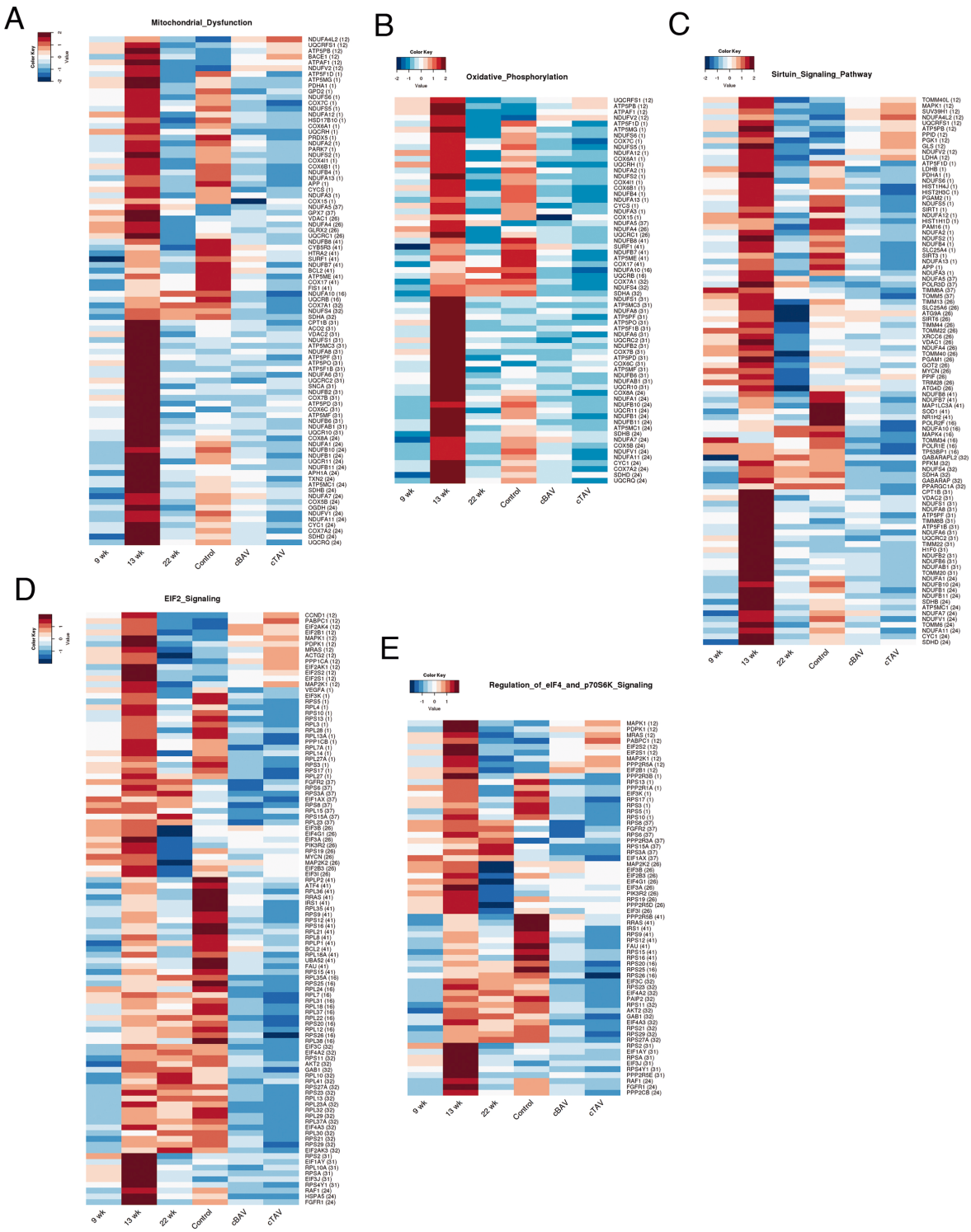

Supplementary_Figure_S8_MacGrogan_et_al

Supplementary Figure S9. (A) Hierarchical clustering of enriched pathways in MC1. IPA results for MC6 identified 7 enriched canonical pathways with a Benjamini-Hochberg adjusted $P<0.05$, which appear listed on the right. The central heatmap represents the percentage of genes shared between pathways (from 0% to 100%). The dendrogram at the top represents pathway relatedness, calculated on the basis of the shared-gene ratio. The heatmap on the left represents mean gene expression for the genes associated with each pathway across biological conditions, on a normalised scale (from -2 to 2, for values below and above the mean, respectively). (B) Top 5 pathways associated with MC1 (C) The single top pathway associated with MC5. Pathways summarized in Figure 3 are involved in cell stress and unfolded protein response. Heatmaps represent expression values for the genes associated with each pathway across biological conditions, on a normalised scale (with negative or positive sign for values below and above the mean, respectively). Gene names and K-means based cluster identifier appear on the right.

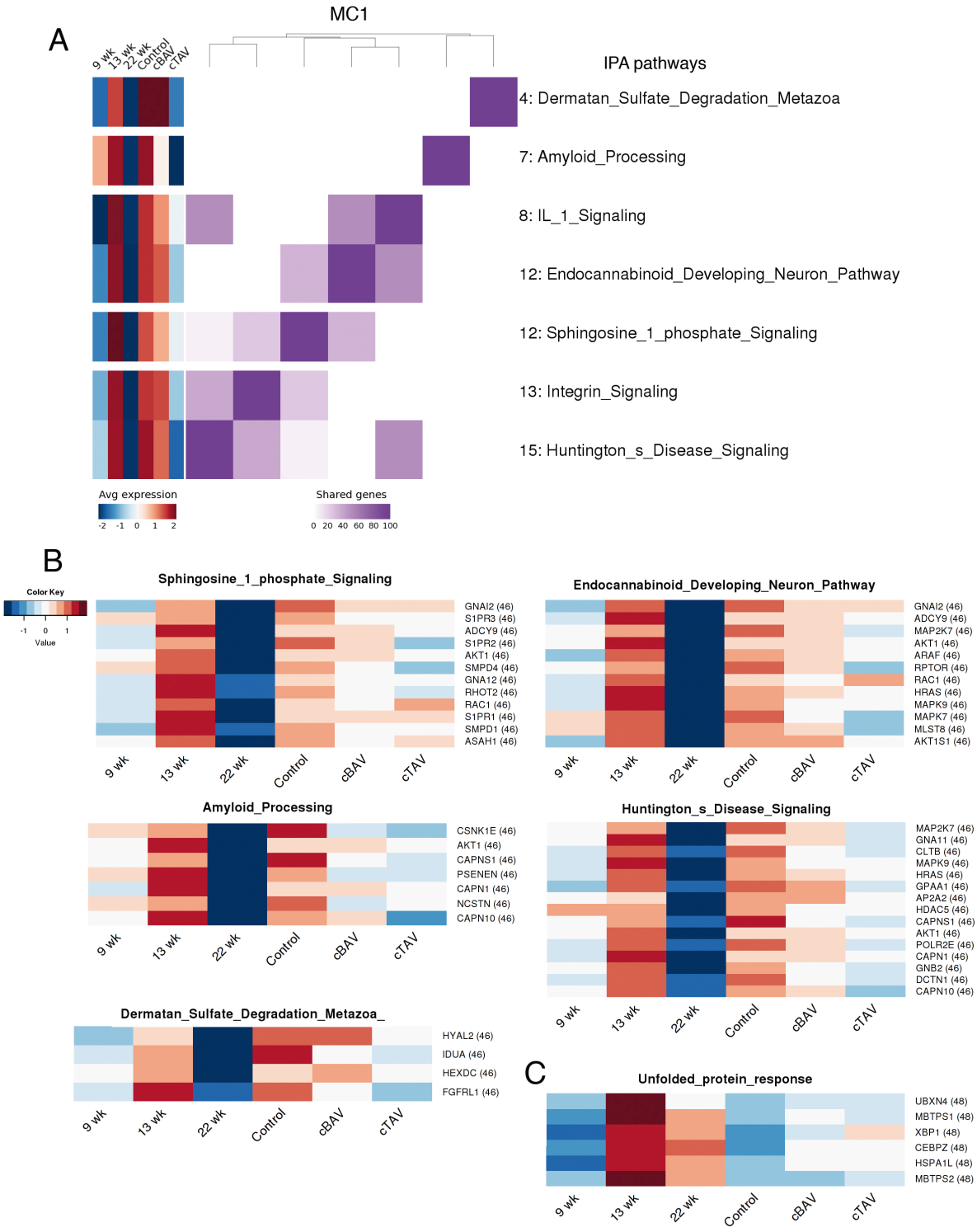

Supplementary_Figure_S9_MacGrogan_et_al

Supplementary Figure S10. (A) Gene expression signature predictive of CAVD. Follow-up after three years. qPCR data (y-axis) vs total coronary calcium (x-axis) for the 6 selected genes in whole blood (WB). Each point represents an individual gene expression level and aortic-valve calcification level. Dots are coloured based on the group to which the individual belongs: CAVD patients (WB-CAVD, n=16), PESA participants with (PESA-SD, n=25) and without (PESA-CTL, n=35) aortic valve calcification. Solid lines represent the linear model fit for PESA-SD and WB-CAVD. Shaded regions represent the confidence of the linear regression estimate for each calcium level. (B) Chronic inflammation drives metabolic stress and premature ageing in CAVD. Diagram describing prominent biological processes and their relationships in CAVD. Chronic inflammation (MC3) is the main process driving CAVD (red arrow, left). The disease passes through a long asymptomatic phase before the onset of CAVD and is modulated by diverse risk factors (left). Cell adhesion and migration (MC4) and cell cycle and DNA repair (MC6) are required during inflammation for the movement and expansion of inflammatory cells. These developmental processes are normally silenced in adult valves but become pathologically reactivated during CAVD (activated processes seen in RNAseq). Chronic inflammation alters cell stress responses (MC2, MC3 and MC5, red boxes), resulting in decreased OXPHOS metabolism and protein translation (MC2) (decreased processes seen in RNA-seq). These changes are associated with age-related neurodegenerative disease (MC1) and premature ageing.

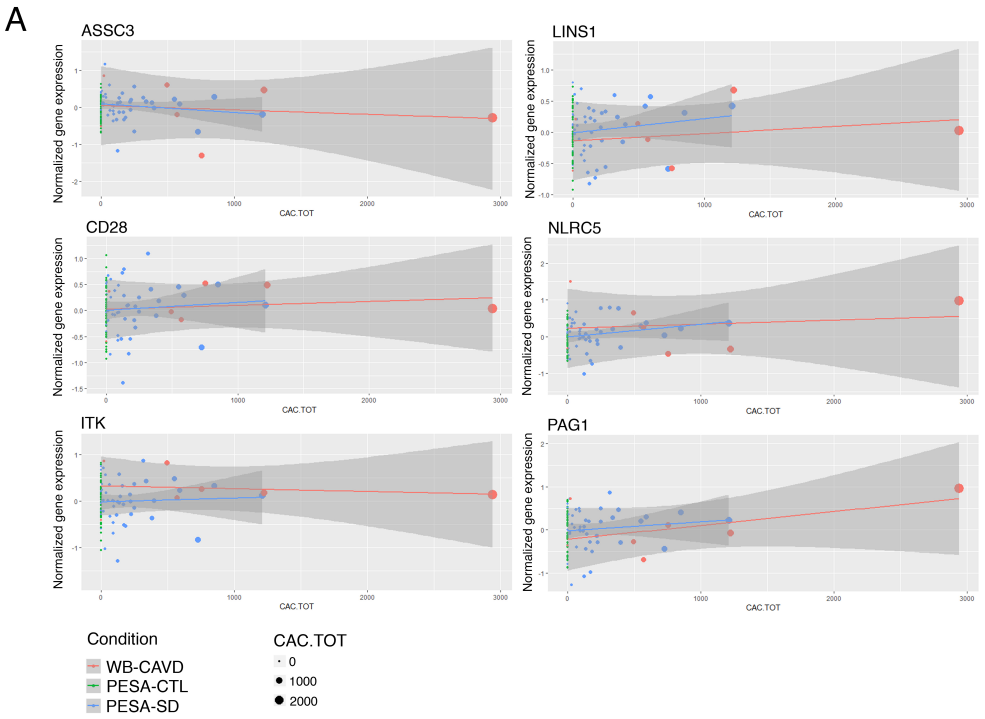

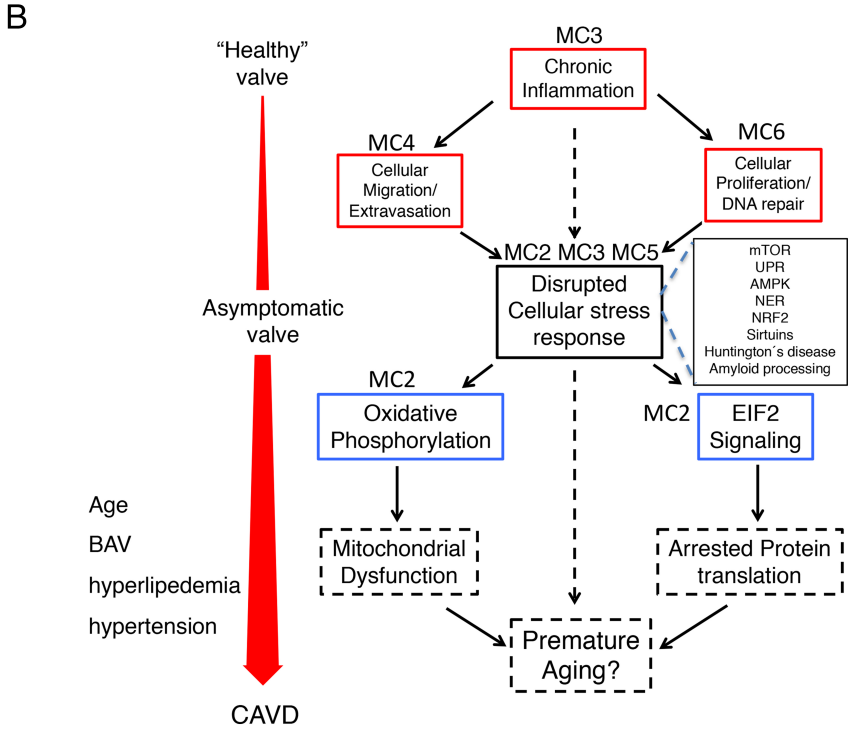

Supplementary Figure S10_MacGrogan_et_al.